Renal denervation reduces atrial remodelling in hypertensive rats with metabolic syndrome

Selejan Simina-Ramona, Linz Dominik, Hohl Mathias, Huynh Anh Khoa Dennis, Mauz Muriel, Wintrich Jan, Kazakov Andrey, Werner Christian, Mahfoud Felix,

Böhm Michael

Klinik für Innere Medizin III (Kardiologie, Angiologie und Internistische Intensivmedizin),

Saarland University, Homburg/Saar, Germany

Correspondance to:
Simina-Ramona Selejan, MD
Klinik für Innere Medizin III

Kirrbergerstr. 100, Geb. 41.1 (IMED)

Universität des Saarlandes
D-66421 Homburg/Saar; Germany
Phone : +49-6841-16-15031
Fax : +49-6841-16-15032
e-mail: simina.selejan@uks.eu

Author contributions: All authors contributed to the study conception and design. Material preparation, data collection and analysis were performed by Selejan Simina-Ramona, Linz Dominik, Huynh Anh Khoa Dennis, Mauz Muriel and Kazakov Andrey. The first draft of the manuscript was written by Selejan Simina-Ramona and all authors commented on previous versions of the manuscript. All authors read and approved the final manuscript. Acknowledgements: The authors thank Laura Frisch for excellent technical assistance.

Funding: This work was supported by HOMFOR 2015/2016 to SRS, the German Heart Foundation (F/03/15 to SRS and DL), the German Research Foundation (Deutsche Forschungsgemeinschaft, SFB/TRR 219 (Project-ID 322900939) to SRS, DL, MH, AK, CW, FM and MB (M02/S02, S01, M06)).

Abstract

Background: Atrial fibrillation (AF) is highly prevalent in hypertensive patients with metabolic syndrome and is related to inflammation and activation of the sympathoadrenergic system. The multi-ligand Receptor-for-Advanced-Glycation-End-products (RAGE) activates inflammation associated tissue remodelling and is regulated by the sympathetic nervous system. Its counterpart, soluble RAGE (sRAGE), serves as anti-inflammatory decoy receptor with protective properties.

Methods and results: We investigated the effect of sympathetic modulation by renal denervation (RDN) on atrial remodelling, RAGE/sRAGE and RAGE-ligands in metabolic syndrome. RDN was performed in spontaneously hypertensive obese rats (SHRob) with metabolic syndrome compared with lean spontaneously hypertensive rats (SHR) and with normotensive non-obese control rats. Blood pressure and heart rate were measured by telemetry. The animals were sacrificed 12 weeks after RDN. Left atrial (LA) remodelling was assessed by histological analysis, collagen types, RAGE/sRAGE and RAGE-ligands expressions were analysed by western blot and immunofluorescence staining. RAGE was increased (+718%) and sRAGE decreased (-62%) in SHRob as compared with controls. RDN reduced RAGE expression (-61% versus SHRob), significantly increased sRAGE levels (+162%) and induced a significant decrease in RAGE-ligand levels in SHRob (-57% CML and -51% HMGB1) with reduced pro-inflammatory NFkB activation (-96%). This led to a reduction in atrial fibrosis (-33%), collagen type I content (-72%), accompanied by reduced LA myocyte hypertrophy (-21%).

Conclusion: Suppression of renal sympathetic nerve activity by RDN prevents atrial remodelling in metabolic syndrome by modulating RAGE/sRAGE balance and reducing pro-inflammatory and pro-fibrotic RAGE ligands, which provides a potential therapeutic mechanism to reduce the development of AF.

Introduction

The prevalence of atrial fibrillation (AF) in patients with metabolic syndrome is elevated compared to non-affected individuals [**31**]. Insights into the mechanisms are sparse [**37**]. However, it is known that metabolic syndrome is associated with increased sympathetic activity, which in turn is associated with a higher risk for AF [**6**]. Renal Denervation (RDN) can modulate sympathetic activation and is currently under investigation as a device-based hypertension treatment [**47**].

Receptor-for-Advanced-Glycation-End-products (RAGE) is a multi-ligand receptor responsible for pro-inflammatory and pro-fibrotic responses in several cardiovascular pathologies, diabetes and metabolic syndrome [**10, 12**]. Proteases [**33, 51**] cleave it to the soluble RAGE (sRAGE), which antagonizes RAGE effects by neutralizing RAGE ligands and also via blocking RAGE itself [**35**]. Increased plasma levels of sRAGE are associated with a reduction in AF recurrence after pulmonary vein isolation in diabetic patients [**20, 50**] and inhibitors of AGE formation have been shown to prevent atrial structural remodelling in diabetic rat models [**19, 53**]. In previous studies, RDN prevented left ventricular interstitial remodelling in a rat model with metabolic syndrome, hypertension and with coexistent renal insufficiency (Spontaneously Hypertensive Obese rats, SHRob) [**24, 38**]. The SHRob carries a mutation of the leptin receptor, leading to receptor dysfunction and leptin resistance [**42**] with increasing obesity, hyperinsulinemia and hyperlipidemia beside hypertension. RDN re-established the left ventricular and serum RAGE/sRAGE balance in these rats. In addition, electrophysiological and structural remodelling of the atria makes such rats with metabolic syndrome prone to AF development [**14**].

Whether changes in atrial RAGE/sRAGE balances can be attained by RDN and whether this influences atrial structural remodelling processes is unknown. Hence, the present study aimed to characterize the influence of the sympathoadrenergic system and its modulation by RDN on atrial interstitial remodelling and on regulation of the RAGE/sRAGE-system and its ligands in metabolic syndrome.

Material and Methods

Reagents

M199 medium and FCS (fetal calf serum) were purchased from Gibco/Invitrogen (Karlsruhe, Germany), Penicillin/streptomycin and ß-adrenergic receptor selective antagonists CGP20712A (C231), ICI118.551 (I127) and isoproterenol (I6504) from Sigma-Aldrich (Deisenhofen, Germany). Primary antibodies against the extracellular domain of human RAGE (ab37647), HMGB1 (ab18256), CML (ab27684) and NFkB (ab28856 and ab131485) were from Abcam (Cambridge, UK), against collagen type I from Southern Biotech (1310-01, Southern Biotech, Birmingham, US). HRP-conjugated secondary antibodies and all other substances used were from Sigma-Aldrich (Deisenhofen, Germany), unless specified otherwise.

Animals

Male 10-week-old obese spontaneously hypertensive (SHRs-ob; n = 12), lean spontaneously hypertensive rats (SHR; n=6) and normotensive Sprague-Dawley rats (controls (Ctrs); n = 6) were purchased from Charles River (Sulzfeld, Germany). At the age of 34 weeks, surgical and chemical renal denervation (RDN) was performed in 6 SHRob as described below. At this age, SHRob had fully established a metabolic syndrome with arterial hypertension, hyperinsulinemia, hyperlipidemia and renal insufficiency. SHRob + RDN (n=6) were compared with 6 sham operated SHRob (SHRob), normotensive controls (Ctr) and lean SHR. The animals were kept in standard cages for the duration of the study and received a standard Chow diet (standard diet No. 1320; Altromin, Lage, Germany) and tap water ad libitum. The animals were sacrificed 12 weeks after RDN. All experiments were performed in accordance with the National Health Guideline for the Care and Use of Laboratory Animals as well as with the Animal Welfare Guidelines and the German law for the protection of animals. The approval of the responsible regional animal ethics committee was obtained.

Renal denervation

At the age of 34 weeks, surgical and chemical RDN was performed in 6 SHRob as previously described [**24**]. Shortly, the rats were anesthetized with 2.5% isoflurane and medial laparotomies with peritoneal incisions were performed to approach both kidneys. All visible nerves were cut in the areas of the renal hili, followed by additional stripping of the adventitia from the renal artery to remove remaining nerve fibers. Finally, the renal arteries were moistened with a 20% phenol/ethanol solution for 10-15 minutes. Sham operations included only kidney exposition without intervention (performed on Ctrs, SHR and SHRob without RDN). Simultaneously to RDN and the sham operations, telemetric sensors were implanted for systolic, diastolic pressure and heart rate acquisition as described before [**24**].

Blood and tissue sampling

The rats were sacrificed at the age of 46 weeks under deep general anaesthesia with isoflurane, xylazine (Rompun®) and ketamine (Ketavet®). Blood was extracted from the aorta and urine from the urinary bladder and stored at -80°C for further analysis. Hearts were quickly excised and atrial tissue was either transferred to 4% paraformaldehyde for histological analysis or was snap-frozen in liquid nitrogen and stored at -80°C for further analysis. Norepinephrine was measured in kidney tissue by high-pressure-liquid-chromatography (HPLC) as described before [**24**].

Histological analysis

Left atrial (LA) tissue was soaked in buffered 4% paraformaldehyde for 24 hours and subsequently embedded in paraffin for further histological analysis. LA sections of 3um thickness were prepared, deparaffined, rehydrated and stained with hematoxylin and eosin (HE) or Picro-Sirius red for further analysis. The Picro-Sirius-Red staining was used for visualization of interstitial and perivascular fibrosis. The percentage of interstitial collagen was given by the image analysis software (Nicon Instruments Software (NIS)-Elements (BR 3.2) as the ratio of the area positively stained with Picro-Sirius red to the total LA area. Additionally, Picro-Sirius red stained sections were additionally analyzed by polarized microscopy for distribution of collagen type I (red-yellow birefringence) and collagen type III (green birefringence). Furthermore, LA sections were additionally stained with hematoxylin and eosin. One hundred cells were measured to determine the cardiomyocyte cellular area in LA sections.

Immunoblotting

Left atrial samples were homogenized with buffer (in mmol/l: Tris 5, EDTA 1, MgCl2 5, pH 8.0, PMSF 1, Leupeptin 1; Aprotinin 5 ug/ml) and mixed 2:1 v/v with SDS-PAGE loading buffer. After denaturation (95°C, 5 min; except for collagen type I western blots, where samples were not denaturated), the samples were separated on 10-12% SDS polyacrylamide electrophoresis gels (25 ug tissue/lane) and transferred to nitrocellulose membranes (Protran®, Schleicher & Schuell GmbH, Dassel, Germany) by semi-dry electrophoretic blotting (0.8 mA/cm2). After blocking with 0.1% Western Blocking Reagent (Roche, Mannheim, Germany) membranes were incubated with primary antibodies for RAGE/sRAGE (ab37647, rabbit polyclonal to RAGE, 1:1000 dilution, Abcam, Cambridge, UK), HMGB1 (ab18256, rabbit polyclonal to HMGB1, 1:1000, Abcam), CML (ab 27684, rabbit polyclonal to CML, 1:2000, Abcam), collagen type I (1310-01, goat anti collagen type I, 1:1000, Southern Biotech), NFkBp65 phospho (ab28856, rabbit polyclonal to NFkBp65 (phospho S536) 1:1000, Abcam) and total NFkBp65 (ab131485, rabbit polyclonal to NFkB p65, 1:1000, Abcam) at 4°C for 12-16h. The respective secondary antibodies were incubated for 60 min at RT and used at a dilution of 1:10000. Proteins were visualized by enhanced chemiluminescence (Amersham Pharmacia Biotech, Freiburg, Germany). Membranes were stripped afterwards for GAPDH analysis as loading control: twice stripped for 15 minutes at 56°C with stripping

buffer (62.5 nM Tris-HCl (pH 6.8), 2%SDS, 0.1 M 2-mercaptoethanol), followed by repeated wash steps with PBS (in mmol/L: NaCl 170, KCl 33, Na2HPO4 40 and KH2PO4 18, pH 7.2), then blocked again in PBS with 5% nonfat dry milk for 120 min at room temperature. Membranes incubated for phospho-NFkB were stripped for total NFkB. Autoradiographs were quantified by imaging densitometry and analysed by the "LabWorks 4.6"Software (LabWorks Image Acquisition and Analysis Software, UVP BioImaging Systems, Cambridge, UK). Data are presented as arbitrary units (AU) normalized to GAPDH and a control sample.

Culture conditions of rat cardiomyofibroblasts (H9C2 cell line)

H9C2-cardiomyoblasts (rattus norvegicus) were purchased from ATCC (ATCC CRL 1446, Wesel, Germany; lot number 3426889) and cultured on uncoated 6well-dishes in 2ml DMEM medium +10%FBS in humidified air (5% CO2, 37°C). After reaching 80% confluency, low FBS medium was added to the cells and stimulation experiments with isoproterenol +/- ß-adrenergic receptor antagonists were performed.

Every 24 hours the cells were stimulated with isoproterenol (0.1 umol/l) in the presence or absence of ß-adrenergic receptor antagonists with differing selectivity (ß1-selective CGP 201712A, ß2-selective ICI 118.551) for a total stimulation period of 72 hours. The ß-blocker was added 30 min prior to isoproterenol. The cell culture supernatant of the stimulated H9C2 cells was asserved every 24 hours and analyzed for sRAGE release. The cells were harvested after 72 hours of stimulation and processed for cell fractionation: The cell pellets were resuspended in hypotonic buffer (in mmol/l: Tris 5, EDTA 1, MgCl2 5, pH 8.0, PMSF 1, Leupeptin 1; Aprotinin 5 ug/ml), incubated for 15 minutes at 4°C, then subjected to 100000 g ultracentrifugation (1h, 4 °C) to obtain a "cytosolic" and "membranous" fraction (pellet). The membrane fraction was resuspended in hypotonic buffer. Membrane fraction and cell culture medium were analyzed for RAGE/sRAGE content by Western blot analysis. The uniform total protein loading on the gel (50 µg/lane) was controlled by Ponceau Red staining (Dianova, Germany). The data are presented as arbitrary units (AU) in percent of a control, unless otherwise stated.

Statistical analysis

Results are presented as mean±SEM. Significance was estimated with Two-way-ANOVA with Tukey´s post hoc test for multiple comparisons. Normal distribution of data was tested by Kolmogorov-Smirnov and Liliefors test. A $p<0.05$ was considered significant. GraphPadPrism (version 6.0; GraphPad Software, San Diego California, USA) was used for statistical analysis.

Results

Metabolic and hemodynamic parameters

Metabolic and ventricular hemodynamic characterizations of the SHRob and SHR models have been recently published [**22, 24**]. SHRob showed significantly increased body weight compared with SHR and controls. Telemetry analysis revealed similarly increased systolic blood pressure in SHR and SHRob versus controls, while heart rate was lower in SHRob and SHR. Fasting serum insulin levels were elevated in SHRob with still normal glycated haemoglobin. Triglycerides and cholesterol were also elevated in SHRob (Table 1).

The effectiveness of renal denervation was indicated by significantly decreased levels of kidney norepinephrine levels. RDN significantly decreased systolic arterial blood pressure and improved kidney function, evoked a numerical, albeit not statistically significant decrease in serum insulin levels and had no effect on lipid levels or body weight (Table 1).

LA structural and interstitial remodelling

SHRob showed increased cardiomyocyte cell area (Table 1; Fig. 1a-b; 131±5.4 um^2 myocyte cell area in SHRob, p=0.0013 versus Ctr and p=0.002 versus SHR). RDN had anti-hypertrophic effects by almost normalizing atrial myocyte size (101±3.4 um^2 in SHRobRDN, p=0.005 versus SHRob). Interstitial collagen deposition (Table 1; Fig. 1c-d) was only numerically augmented in SHR, but strongly increased in SHRob (22.2±1.8% in SHRob versus 5.5±0.3% in Ctr, p<0.001) and significantly decreased after RDN (14.8±1.8% in SHRobRDN versus 22.2±1.8% in SHRob, p=0.02). Additionally, SHRob rats demonstrated a shift to collagen type I (red-yellow fibers) as assessed by polarization microscopy (Table 1; Fig. 1e-f), the collagen type I/collagen type III ratio being normalized after RDN. Western blot analysis for collagen type I protein expression (Table 1; Fig. 1g) confirmed significantly increased collagen type I protein content in SHRob (4±1 AU/GAPDH in SHRob versus 0.9±0.2 AU/GAPDH in Ctr, p=0.004; 1.5±0.3 AU/GAPDH in SHR, p=0.02 versus SHRob), which was reduced after RDN (1.1±0.1 AU/GAPDH in SHRobRDN versus 4±1 AU/GAPDH in SHRob, p=0.007).

LA RAGE/sRAGE regulation

Assessment of LA RAGE protein expression showed a significant up-regulation in SHRob (Table 1; Fig. 2a-b; 3.6±0.7 AU/GAPDH in SHRob versus 0.4±0.05 in Ctr, p=0.001). RDN induced a significant reduction in LA content of full-length RAGE in the SHRobRDN group (1.4±0.3 AU/GAPDH, p=0.016 versus SHRob). LA sRAGE content was significantly decreased in SHRob as compared to Ctr (Fig. 2c, 2.5±0.8 AU/GAPDH in SHRob versus 6.4±0.3 AU/GAPDH in Ctr, p=0.04) while in SHRobRDN sRAGE levels were significantly augmented (6.5±0.9 AU/GAPDH, p=0.02 versus SHRob).

RDN decreases levels of RAGE-ligands CML and HMGB1 in atrial tissue.

Left atrial CML levels (Table 1; Fig. 3a) were increased in SHR (3.6±0.7 AU/GAPDH) and SHRob (4.6±1.1 AU/GAPDH) versus controls (0.9±0.1 AU/GAPDH in Ctr, p=0.005 versus SHRob and p=0.04 versus SHR) and attenuated after RDN (2.0±0.3 AU/GAPDH, p=0.03 versus SHRob).

SHRob further demonstrated significantly increased left atrial HMGB1 levels as compared with SHR and controls (Table 1; Fig. 3b; 4.5±0.6 AU/GAPDH in SHRob versus 1.8±0.1 in SHR and 1.5±0.4 in Ctr, p=0.0003-0.0006 for each comparison). Again, RDN treatment resulted in a significant reduction of LA HMGB1 protein levels (Fig. 3b; 2.2±0.2 AU/GAPDH in SHRobRDN, p=0.002 versus SHRob), achieving similarly low levels as in SHR (1.8±0.1 AU/GAPDH) and controls alone (1.5±0.4 AU/GAPDH).

The phospho-NFkB/total NFkB-ratio, representative of a partially RAGE-induced pro-inflammatory status, was increased in SHRob (Table 1; Fig. 3c: 3.4±0.9 in SHRob versus 0.16±0.04 in Ctr, p=0.001) and was normalized after RDN (0.14±0.05 in SHRobRDN versus 3.4±0.9 in SHRob, p=0.001, and p>0.05 versus 0.16±0.04 in Ctr).

In vitro ß-adrenergic stimulation of H9C2 cells increases RAGE expression and decreases sRAGE secretion.

H9C2 cells were repeatedly stimulated with the ß1+ß2-adrenoreceptor agonist isoproterenol (0.1 µmol/l every 24 hours), which lead to a significant increase in RAGE content in the cell membrane (+129%) (Fig. 4a)). Simultaneously, sRAGE shedding into the cell culture medium was reduced by isoproterenol treatment (-36% (Fig. 4b)). To identify the ß-adrenergic receptor subtype involved, we also used ß-adrenergic receptor antagonists with different selectivity (CGP 201712A (ß1-selective) or ICI 118.551 (ß2-selective)) simultaneously to isoproterenol stimulation. The isoproterenol-induced RAGE expression (Fig. 4a) was reversed by the ß1-adrenergic receptor blockade with CGP, while sRAGE shedding recovered with ß2-adrenergic receptor blockade by ICI (Fig. 4b).

Discussion

This study shows that RDN effectively inhibits atrial remodelling in metabolic syndrome. Interstitial fibrosis is a characteristic of atria, prone to develop AF [**17**]. Herein, we documented increased interstitial fibrosis in the LA of hypertensive rats with metabolic syndrome. RDN effectively inhibited atrial remodelling and reduced atrial fibrosis in these rats. Considering the polarized microscopy and western blot analyses for collagen type I, the main part of the fibrosis appeared to be caused by an increase in type I collagen with augmented collagen type I/collagen type III ratio. This collagen-shift has been studied in left ventricular stiffness [**11**], but also in atrial remodelling, where an augmented collagen type

I/type III ratio in patients undergoing heart surgery was associated with an increased risk for postoperative atrial fibrillation [**13**].

Also, RAGE is known to increase collagen type I transcription [**32**]. We observed a shift in RAGE/sRAGE balance with increased RAGE and decreased sRAGE in the left atria of sham-operated SHRob, matching the pro-fibrotic changes. RAGE/sRAGE was brought to a more favourable ratio following neuromodulation via RDN. As shown by the in-vitro experiments, these effects are partly independent of systemic blood pressure, but can be induced by sole ß-adrenergic activation. The observations extend previous results [**38**], where a ß-adrenergic-induced in-vitro RAGE/sRAGE regulation in cardiac fibroblasts and peripheral blood mononuclear cells was demonstrated. We could reproduce those results herein with rat cardiomyoblastoma cells (H9C2 cell line).

Additionally, increased levels of RAGE ligands were observed in left atria of SHRob. It is known that RAGE activation by RAGE ligands increases oxidative stress and inflammation, which in turn leads to an increased formation of RAGE ligands and transcription of RAGE protein, in the sense of a vicious circle [**15**]. CML is a major advanced glycation end product and is not only increased in diabetes [**36**], but also associated with an early development of hypertension [**2**]. In this study, atrial CML levels were increased both in SHRob and SHR. Similar CML regulations in serum and left ventricular myocardium in this rat model were reported previously [**38**]. In addition, deposits of AGEs not only promote fibrosis formation by e.g. RAGE-mediated inflammation and collagen production, but also inhibit collagenase mediated collagen degradation by cross-linking the fibrils, making fibrosis more persistent [**3, 54**]. HMGB1, another RAGE-ligand and alarmin molecule, is released by activated immune cells or necrotic cells [**27**].

Recent data suggest that HMGB1 acts as an adipokine in metabolic syndrome [**39, 52**] and plays a central role in the pathogenesis of insulin resistance [**45**]. Corresponding to a systemic effect, atrial HMGB1 content was also increased solely in obese animals, and in left ventricular myocardium and serum according to previous findings [**38**]. An increase in atrial HMGB1 tissue concentration is of particular interest, as HMGB1 is also associated with pro-thrombotic states [**9**] and intra-cardiac thrombus formation by activating platelets [**48**]. Atrial HMGB1 was normalized after RDN in this study, providing evidence for a systemic sympathoadrenergic mediated HMGB1 regulation in metabolic syndrome. Inflammatory mechanisms are known to induce atrial arrhythmias and to promote the development of persistent atrial fibrillation [**7**]. Both CML and HMGB1 were increased in left atrial tissue in metabolic syndrome, indicating activation of RAGE with consecutive activation of pro-inflammatory signal transduction pathways. In line with this hypothesis, the NFkB signal transduction pathway was activated in atria of SHRob, which was significantly decreased after RDN.

The rat model used herein comprises multiple concomitant risk factors, which might exacerbate atrial structural remodelling including arterial hypertension [**21**], obesity with hyperinsulinemia [**28**], and chronic kidney disease [**40, 46**]. All these conditions are known to be associated with a RAGE/sRAGE imbalance [**19, 34**], contributing to atrial maladaptive

remodelling processes [**29, 53**]. The association between increased sympathetic nerve activity and high prevalence of atrial fibrillation has been well demonstrated [**23, 25-26**]. The activation of the sympathetic nervous system plays an important role in the initiation and perpetuation of atrial fibrillation under various pathophysiological conditions [**37**] by structural and electrophysiological changes [**16, 44, 49**]. In a previous report using the same rat model for metabolic syndrome, several aspects of atrial remodelling were demonstrated, such as impaired LA-emptying function and increased propensity of atrial fibrillation as a consequence of electrophysiological and structural remodelling [**14**].

Catheter-based RDN is currently being utilized for treatment of uncontrolled hypertension [**4-5**]. Recently published randomized, sham-controlled clinical trials [**1, 18**] have provided the proof of concept for the blood pressure-lowering efficacy of this approach. A growing body of evidence suggests, that catheter-based RDN may also be used in patients with cardiac arrhythmias [**8, 41, 43**]. In a randomized controlled study in 302 patients with paroxysmal atrial fibrillation and hypertension, renal denervation added to pulmonary vein isolation, compared with catheter ablation alone, significantly increased the likelihood of freedom from atrial fibrillation at 12 months [**41**]. Our findings extend these data by showing that RDN could represent an alternative therapy in atrial fibrillation by inhibiting atrial interstitial remodelling and atrial RAGE/sRAGE dysbalance as well as inflammation in metabolic syndrome.

Limitations

The animal model for metabolic syndrome includes several individual risk factors and pathologies, i.e. hypertension, disturbed glucose tolerance or renal dysfunction. Each of those could have impacted some of the observations made. From clinical studies we know that aggressive risk factor management improves long-term success of AF ablation [**30**]. We aimed to investigate the impact of arterial hypertension alone on the overall picture of the metabolic syndrome regarding atrial RAGE/sRAGE regulation and atrial remodelling by including the SHR group in our study. However, further detailed investigations on obesity, diabetes and renal failure models alone are necessary to characterize the intricate network of pathologies and the influence of the sympathetic nervous system on atrial structural remodelling in each context.

Conclusion

Sympathoadrenergic activation in metabolic syndrome worsens RAGE/sRAGE balance leading to interstitial remodelling and damage in the left atrium. Renal denervation improves atrial interstitial remodelling with restored RAGE/sRAGE balance, reduced RAGE ligands and exhibits anti-inflammatory, anti-hypertrophic and anti-fibrotic effects. Our results can help to establish new therapeutic targets and strategies to improve and prevent atrial fibrillation in metabolic syndrome.

……

Funding

This work was supported by HOMFOR 2015/2016 to SRS, the German Heart Foundation (F/03/15 to SRS and DL), the German Research Foundation (Deutsche Forschungsgemeinschaft, SFB/TRR 219 (Project-ID 322900939) to SRS, DL, MH, AK, CW, FM and MB (M02/S02, S01, M06)).

Acknowledgements

The authors thank Laura Frisch for excellent technical assistance.

Conflict of interest

M.B. has received speaker honoraria for lectures and scientific advice from Abbott, AstraZeneca, Boehringer Ingelheim, Medtronic, Servier, Vifor and Novartis outside of the submitted work. FM is supported by Deutsche Gesellschaft für Kardiologie (DGK) and has received scientific support and speaker honoraria from Bayer, Boehringer Ingelheim, Medtronic and ReCor Medical. The other authors have no conflicts of interest to declare that are relevant to the content of this article.

References

1. Azizi M, Schmieder RE, Mahfoud F, Weber MA, Daemen J, Davies J, Basile J, Kirtane AJ, Wang Y, Lobo MD, Saxena M, Feyz L, Rader F, Lurz P, Sayer J, Sapoval M, Levy T, Sanghvi K, Abraham J, Sharp ASP, Fisher NDL, Bloch MJ, Reeve-Stoffer H, Coleman L, Mullin C, Mauri L; RADIANCE-HTN Investigators (2018) Endovascular ultrasound renal denervation to treat hypertension (RADIANCE-HTN SOLO): a multicentre, international, single-blind, randomised, sham-controlled trial. Lancet. 391: 2335-2345. doi: 10.1016/S0140-6736(18)31082-1

2. Baumann M, Stehouwer C, Scheijen J, Heemann U, Struijker Boudier H, Schalkwijk C (2008) N epsilon-(carboxymethyl)lysine during the early development of hypertension. Ann N Y Acad Sci. 1126: 201-204. doi: 10.1196/annals.1433.004

3. Begieneman MP, Rijvers L, Kubat B, Paulus WJ, Vonk AB, van Rossum AC, Schalkwijk CG, Stooker W, Niessen HW, Krijnen PA (2015) Atrial fibrillation coincides with the advanced glycation end product N(ε)-(carboxymethyl)lysine in the atrium. Am J Pathol. 185: 2096-2104. doi: 10.1016/j.ajpath.2015.04.018

4. Böhm M, Linz D, Urban D, Mahfoud F, Ukena C (2013) Renal sympathetic denervation: applications in hypertension and beyond. Nat Rev Cardiol. 10: 465-476. doi: 10.1038/nrcardio.2013.89

5. Böhm M, Mahfoud F, Ukena C, Hoppe UC, Narkiewicz K, Negoita M, Ruilope L, Schlaich MP, Schmieder RE, Whitbourn R, Williams B, Zeymer U, Zirlik A, Mancia G; GSR Investigators. (2015) First report of the Global SYMPLICITY Registry on the effect of renal artery denervation in patients with uncontrolled hypertension. Hypertension. 65: 766-774. doi: 10.1161/HYPERTENSIONAHA.114.05010

6. Carnagarin R, Kiuchi MG, Ho JK, Matthews VB, Schlaich MP (2019) Sympathetic nervous system activation and its modulation: role in atrial fibrillation. Front Neurosci. 12: 1058. doi: 10.3389/fnins.2018.01058

7. Chung MK , Martin DO, Sprecher D, Wazni O, Kanderian A, Carnes CA, Bauer JA, Tchou PJ, Niebauer MJ, Natale A, Van Wagoner DR (2001) C-reactive protein elevation in patients with

atrial arrhythmias: inflammatory mechanisms and persistence of atrial fibrillation. Circulation. 104: 2886-2891. doi: 10.1161/hc4901.101760

8. Donazzan L, Mahfoud F, Ewen S, Ukena C, Cremers B, Kirsch CM, Hellwig D, Eweiwi T, Ezziddin S, Esler M, Böhm M (2016) Effects of catheter-based renal denervation on cardiac sympathetic activity and innervation in patients with resistant hypertension. Clin Res Cardiol. 105: 364-371. doi: 10.1007/s00392-015-0930-4

9. Dyer MR, Chen Q, Haldeman S, Yazdani H, Hoffman R, Loughran P, Tsung A, Zuckerbraun BS, Simmons RL, Neal MD (2018) Deep vein thrombosis in mice is regulated by platelet HMGB1 through release of neutrophil-extracellular traps and DNA. Sci Rep. 8: 2068. doi: 10.1038/s41598-018-20479-x

10. Egaña-Gorroño L, López-Díez R, Yepuri G, Ramirez LS, Reverdatto S, Gugger PF, Shekhtman A, Ramasamy R, Schmidt AM (2020) Receptor for Advanced Glycation End Products (RAGE) and mechanisms and therapeutic opportunities in diabetes and cardiovascular disease: insights from human subjects and animal models. Front Cardiovasc Med. 10; 7: 37. doi: 10.3389/fcvm.2020.00037

11. Eiros R, Romero-González G, Gavira JJ, Beloqui O, Colina I, Fortún Landecho M, López B, González A, Díez J, Ravassa S (2020) Does chronic kidney disease facilitate malignant myocardial fibrosis in heart failure with preserved ejection fraction of hypertensive origin? J Clin Med. 9. doi: 10.3390/jcm9020404

12. Goova MT, Li J, Kislinger T, Qu W, Lu Y, Bucciarelli LG, Nowygrod S, Wolf BM, Caliste X, Yan SF, Stern DM, Schmidt AM (2001) Blockade of receptor for advanced glycation end-products restores effective wound healing in diabetic mice. Am J Pathol. 159: 513-525. doi: 10.1016/S0002-9440(10)61723-3

13. Grammer JB, Böhm J, Dufour A, Benz M, Lange R, Bauernschmitt R (2005) Atrial fibrosis in heart surgery patients: decreased collagen III/I ratio in postoperative atrial fibrillation. Basic Res Cardiol. 100: 288-294. doi: 10.1007/s00395-005-0515-x

14. Hohl M, Lau DH, Müller A, Elliott AD, Linz B, Mahajan R, Hendriks JML, Böhm M, Schotten U, Sanders P, Linz D (2017) Concomitant obesity and metabolic syndrome add to the atrial arrhythmogenic phenotype in male hypertensive rats. J Am Heart Assoc. 6; e006717. doi: 10.1161/JAHA.117.006717

15. Hudson BI, Lippman ME (2018) Targeting RAGE signaling in inflammatory disease. Annu Rev Med. 69: 349-364. doi: 10.1146/annurev-med-041316-085215

16. Huiliang Q, Chunlan J, Wei L, Yuchi W, Zhaoyu L, Qizhan L, Zheng X, Xusheng L, Huanlin W, Wei J, Chuan Z (2018) Chronic kidney disease increases atrial fibrillation inducibility: involvement of inflammation, atrial fibrosis, and connexins. Front Physiol. 9: 1726. doi: 10.3389/fphys.2018.01726.

17. Jalife J, Kaur K (2015) Atrial remodeling, fibrosis, and atrial fibrillation. Trends Cardiovasc Med. 25: 475–484. doi: 10.1016/j.tcm.2014.12.015

18. Kandzari DE, Böhm M, Mahfoud F, Townsend RR, Weber MA, Pocock S, Tsioufis K, Tousoulis D, Choi JW, East C, Brar S, Cohen SA, Fahy M, Pilcher G, Kario K; SPYRAL HTN-ON MED Trial Investigators (2018) Effect of renal denervation on blood pressure in the presence of antihypertensive drugs: 6-month efficacy and safety results from the SPYRAL HTN-ON MED proof-of-concept randomised trial. Lancet. 391: 2346-2355. doi: 10.1016/S0140-6736(18)30951-6

19. Kato T, Yamashita T, Sekiguchi A, Tsuneda T, Sagara K, Takamura M, Kaneko S, Aizawa T, Fu LT (2008) AGEs-RAGE system mediates atrial structural remodeling in the diabetic rat. J Cardiovasc Electrophysiol. 19: 415-420. doi: 10.1111/j.1540-8167.2007.01037.x

20. Lancefield TF, Patel SK, Freeman M, Velkoska E, Wai B, Srivastava PM, Horrigan M, Farouque O, Burrell LM (2016) The receptor for advanced glycation end products (RAGE) is associated with persistent atrial fibrillation. PLoS One. 11: e0161715. doi: 10.1371/journal.pone.0161715

21. Lau DH, Shipp NJ, Kelly DJ, Thanigaimani S, Neo M, Kuklik P, Lim HS, Zhang Y, Drury K, Wong CX, Chia NH, Brooks AG, Dimitri H, Saint DA, Brown L, Sanders P (2013) Atrial arrhythmia in ageing spontaneously hypertensive rats: unraveling the substrate in hypertension and ageing. PLoS One. 8: e72416. doi: 10.1371/journal.pone.0072416.

22. Linz D, Hohl M, Mahfoud F, Reil JC,Linz W, HeubschleT, Juretschke HP, Neumann H, Aflin C, Reutten H, Böhm M (2012) Cardiac remodeling and myocardial dysfunction in obese spontaneously hypertensive rats. J Transl Med. 10: 187. doi: 10.1186/1479-5876-10-187

23. Linz D, Hohl M, Nickel A, Mahfoud F, Wagner M, Ewen S, Schotten U, Maack C, Wirth K, Böhm M (2013) Effect of renal denervation on neurohumoral activation triggering atrial fibrillation in obstructive sleep apnea. Hypertension. 62: 767-774. doi: 10.1161/HYPERTENSIONAHA.113.01728.

24. Linz D, Hohl M, Schutze J, Mahfoud F, Speer T, Linz B, Hubschle T, Juretschke HP, Dechend R, Geisel J, Rutten H, Böhm M (2014) Progression of kidney injury and cardiac remodeling in obese spontaneously hypertensive rats: the role of renal sympathetic innervation. Am J Hypertens. 28: 256-265. doi: 10.1093/ajh/hpu123

25. Linz D, Ukena C, Mahfoud F, Neuberger HR, Böhm M (2013) Atrial autonomic innervation: a target for interventional antiarrhythmic therapy? J Am Coll Cardiol. 63: 215-224. doi: 10.1016/j.jacc.2013.09.020

26. Linz D, van Hunnik A, Hohl M, Mahfoud F, Wolf M, Neuberger HR, Casadei B, Reilly SN, Verheule S, Böhm M, Schotten U (2015) Catheter-based renal denervation reduces atrial nerve sprouting and complexity of atrial fibrillation in goats. Circ Arrhythm Electrophysiol. 8: 466-474. doi: 10.1161/CIRCEP.114.002453

27. Lotze MT, Tracey KJ (2005) High-mobility group box 1 protein (HMGB1): nuclear weapon in the immune arsenal. Nat Rev Immunol. 5: 331-342. doi: 10.1038/nri1594

28. Mahajan R, Lau DH, Brooks AG, Shipp NJ, Manavis J, Wood JP, Finnie JW, Samuel CS, Royce SG, Twomey DJ, Thanigaimani S, Kalman JM, Sanders P (2015) Electrophysiological, electroanatomical, and structural remodeling of the atria as consequences of sustained obesity. J Am Coll Cardiol. 66: 1–11. doi: 10.1016/j.jacc.2015.04.058

29. McManus DD, Saczynski JS, Ward JA, Jaggi K, Bourrell P, Darling C, Goldberg RJ (2012) The relationship between atrial fibrillation and chronic kidney disease: epidemiologic and pathophysiologic considerations for a dual epidemic. J Atr Fibrillation. 5: 442. doi: 10.4022/jafib.442

30. Pathak RK, Middeldorp ME, Lau DH, Mehta AB, Mahajan R, Twomey D, Alasady M, Hanley L, Antic NA, McEvoy RD, Kalman JM, Abhayaratna WP, Sanders P (2014) Aggressive

risk factor reduction study for atrial fibrillation and implications for the outcome of ablation: the ARREST-AF cohort study. J Am Coll Cardiol. 64: 2222–2231.
doi: 10.1016/j.jacc.2014.09.028

31. Pathak RK, Middeldorp ME, Meredith M, Mehta AB, Mahajan R, Wong CX, Twomey D, Elliott AD, Kalman JM, Abhayaratna WP, Lau DH, Sanders P (2015) Long term effect of goal-directed weight management in an atrial fibrillation cohort: a long-term follow-up study (LEGACY). J Am Coll Cardiol. 65: 2159–2169. doi: 10.1016/j.jacc.2015.03.002

32. Peng Y, Kim JM, Park HS, Yang A, Islam C, Lakatta EG, Lin L (2016) AGE-RAGE signal generates a specific NF-κB RelA "barcode" that directs collagen I expression. Sci Rep. 6: 18822. doi: 10.1038/srep18822

33. Raucci A, Cugusi S, Antonelli A, Barabino SM, Monti L, Bierhaus A, Reiss K, Saftig P, Bianchi ME (2008) A soluble form of the receptor for advanced glycation endproducts (RAGE) is produced by proteolytic cleavage of the membrane-bound form by the sheddase a disintegrin and metalloprotease 10 (ADAM10). FASEB J. 22: 3716-3727. doi: 10.1096/fj.08-109033

34. Santilli F, Blardi P, Scapellato C, Bocchia M, Guazzi G, Terzuoli L, Tabucchi A, Silvietti A, Lucani B, Gioffrè WR, Scarpini F, Fazio F, Davì G (2015) Decreased plasma endogenous soluble RAGE, and enhanced adipokine secretion, oxidative stress and platelet/coagulative activation identify non-alcoholic fatty liver disease among patients with familial combined hyperlipidemia and/or metabolic syndrome. Vascul Pharmacol. 72: 16-24.
doi: 10.1016/j.vph.2015.04.004

35. Sárkány Z, Ikonen TP, Ferreira-da-Silva F, Saraiva MJ, Svergun D, Damas AM (2011) Solution structure of the soluble receptor for advanced glycation end products (sRAGE). J Biol Chem. 286: 37525-37534. doi: 10.1074/jbc.M111.223438

36. Schleicher ED, Wagner E, Nerlich AG (1997) Increased accumulation of the glycoxidation product N(epsilon)-(carboxymethyl)lysine in human tissues in diabetes and aging. J Clin Invest. 99: 457-468. doi: 10.1172/JCI119180

37. Schotten U, Verheule S, Kirchhof P, Goette A (2011) Pathophysiological mechanisms of atrial fibrillation: a translational appraisal. Physiol Rev. 91: 265-325.
doi: 10.1152/physrev.00031.2009

38. Selejan SR, Linz D, Tatu AM, Hohl M, Speer T, Ewen S, Mahfoud F, Kindermann I, Zamyatkin O, Kazakov A, Laufs U, Böhm M (2018) Sympathoadrenergic suppression improves heart function by upregulating the ratio of sRAGE/RAGE in hypertension with metabolic syndrome. J Mol Cell Cardiol. 122: 34-46. doi: 10.1016/j.yjmcc.2018.08.003

39. Shimizu T, Yamakuchi M, Biswas KK, Aryal B, Yamada S, Hashiguchi T, Maruyama I. (2016) HMGB1 is secreted by 3T3-L1 adipocytes through JNK signaling and the secretion is partially inhibited by adiponectin. Obesity (Silver Spring). 24: 1913-1921. doi: 10.1002/oby.21549

40. Soliman EZ, Prineas RJ, Go AS, Xie D, Lash JP, Rahman M, Ojo A, Teal VL, Jensvold NG, Robinson NL, Dries DL, Bazzano L, Mohler ER, Wright JT, Feldman HI; Chronic Renal Insufficiency Cohort (CRIC) Study Group (2010) Chronic kidney disease and prevalent atrial fibrillation: the Chronic Renal Insufficiency Cohort (CRIC). Am Heart J. 159: 1102-1107. doi: 10.1016/j.ahj.2010.03.027

41. Steinberg JS, Shabanov V, Ponomarev D, Losik D, Ivanickiy E, Kropotkin E, Polyakov K, Ptaszynski P, Keweloh B, Yao CJ, Pokushalov EA, Romanov AB (2020) Effect of renal denervation and catheter ablation vs catheter ablation alone on atrial fibrillation recurrence among patients with paroxysmal atrial fibrillation and hypertension: the ERADICATE-AF randomized clinical trial. JAMA. 323: 248-255. doi: 10.1001/jama.2019.21187.

42. Takaya K, Ogawa Y, Hiraoka J, Hosoda K, Yamori Y, Nakao K, Koletsky RJ (1996) Nonsense mutation of leptin receptor in the obese spontaneously hypertensive Koletsky rat. Nat Genet. 14:130-131. doi: 10.1038/ng1096-130

43. Veiga GL, Nishi EE, Estrela HF, Lincevicius GS, Gomes GN, Simões Sato AY, Campos RR, Bergamaschi CT (2016) Total renal denervation reduces sympathoexcitation to different target organs in a model of chronic kidney disease. Auton Neurosci. pii: S1566-0702(16)30269-7. doi: 10.1016/j.autneu.2016.11.006

44. Waldron NH, Fudim M, Mathew JP, Piccini JP (2019) Neuromodulation for the treatment of heart rhythm disorders. JACC Basic Transl Sci. 4: 546-562. doi:10.1016/j.jacbts.2019.02.009

45. Wang Y, Zhong J, Zhang X, Liu Z, Yang Y, Gong Q, Ren B (2016) The role of HMGB1 in the pathogenesis of type 2 diabetes. J Diabetes Res. 2016: 2543268. doi: 10.1155/2016/2543268.

46. Winkelmayer WC, Patrick AR, Liu J, Brookhart MA, Setoguchi S (2011) The increasing prevalence of atrial fibrillation among hemodialysis patients. J Am Soc Nephrol. 22: 349-357. doi: 10.1681/ASN.2010050459

47. Wyatt CM, Textor SC (2018) Emerging evidence on renal denervation for the treatment of hypertension. Kidney Int. 94: 644-646. doi: 10.1016/j.kint.2018.08.002

48. Xu Q, Bo L, Hu J, Geng J, Chen Y, Li X, Chen F, Song J (2018) High mobility group box 1 was associated with thrombosis in patients with atrial fibrillation. Medicine (Baltimore). 97: e0132. doi: 10.1097/MD.0000000000010132

49. Yamada S, Fong MC, Hsiao YW, Chang SL, Tsai YN, Lo LW , Chao TF, Lin YJ , Hu YF, Chung FP , Liao JN, Chang YT, Li HY, Higa S, Chen SA (2018) Impact of renal denervation on atrial arrhythmogenic substrate in ischemic model of heart failure. J Am Heart Assoc. 7: e007312. doi: 10.1161/JAHA.117.007312.

50. Yang PS, Kim TH, Uhm JS, Park S, Joung B, Lee MH, Pak HN (2016) High plasma level of soluble RAGE is independently associated with a low recurrence of atrial fibrillation after catheter ablation in diabetic patient. Europace. 18: 1711-1718. doi: 10.1093/europace/euv449

51. Zhang L, Bukulin M, Kojro E, Roth A, Metz VV, Fahrenholz F, Nawroth PP, Bierhaus A, Postina R (2008) Receptor for advanced glycation end products is subjected to protein ectodomain shedding by metalloproteinases. J Biol Chem. 283: 35507–35516. doi: 10.1074/jbc.M806948200

52. Zhang J, Zhang L, Zhang S, Yu Q, Xiong F, Huang K, Wang CY, Yang P (2017) HMGB1, an innate alarmin, plays a critical role in chronic inflammation of adipose tissue in obesity. Mol Cell Endocrinol. 454: 103-111. doi: 10.1016/j.mce.2017.06.012

53. Zhang Q, Li G, Liu T (2013) Receptor for advanced glycation end products (RAGE): novel biomarker and therapeutic target for atrial fibrillation. Int J Cardiol. 168: 4802-4804. doi: 10.1016/j.ijcard.2013.07.038

54. Zhao J, Randive R, Stewart JA (2014) Molecular mechanisms of AGE/RAGE-mediated fibrosis in the diabetic heart. World J Diabetes. 5: 860-867. doi: 10.4239/wjd.v5.i6.860

Figure Legends

Fig.1

a) Representative histological pictures (hematoxyline eosin staining) and

b) Quantification of LA myocyte cell surface in atrial tissue of normotensive controls (n=5), SHR (n=6), SHRob (n=5) and SHRobRDN (n=5).

c) Representative histological pictures (picrosirius red staining) and

d) Quantification of left atrial fibrotic area (interstitial fibrillar collagen fractional area (%)) in normotensive controls (n=5), SHR (n=6), SHRob (n=5) and SHRobRDN (n=5).

e) Representative images (polarization microscopy) and

f) Assessment of collagen type I (red-yellow birefringence)/collagen type III (green birefringence) ratio in left atrial tissue of normotensive controls (n=5), SHR (n=6), SHRob (n=5) and SHRobRDN (n=5)

g) Representative Western blot (upper panel) and quantification of collagen type I (lower panel) in left atrial homogenates from normotensive controls (n=5), SHR (n=6), SHRob (n=5) and SHRobRDN (n=5). Collagen type I in arbitrary units (AU) normalized to GAPDH. **p<0.05 versus Control; § p<0.05 versus SHR; #p<0.05 versus SHRob*

Fig. 2

a) Representative fluorescence microscopy for RAGE (stained red by TRITC), atrial tissue autofluorescence (green) and nuclei (stained blue by DAPI) in left atria of control rats (left panel), SHR (first middle panel), SHRob (second middle panel) and SHRobRDN rats (right panel) (n=3 each group). Magnification 20x. Scale bar 50 µm**.**

b) Representative Western blot (upper panel) and quantification of left atrial RAGE (lower panel) and

c) sRAGE in left atrial homogenates from normotensive controls (n=5), SHR (n=6), SHRob (n=5) and SHRobRDN (n=5).

RAGE and sRAGE in arbitrary units (AU) normalized to GAPDH. **p<0.05 versus Control; § p<0.05 versus SHR; #p<0.05 versus SHRob*

Fig. 3

a) Representative Western blot of left atrial CML-modified proteins (upper panel) and quantification of left atrial CML in normotensive controls (n=5), SHR (n=6), SHRob (n=5) and SHRobRDN (n=5). CML in arbitrary units (AU) normalized to GAPDH.

The antibody reacts species independently and specifically recognizes carboxymethyllysine modified proteins (Western blot with multiple bands belonging to different proteins).

b) Representative Western blot (upper panel) and quantification of left atrial HMGB1 (lower panel) in homogenates from normotensive controls (n=5), SHR (n=6), SHRob (n=5) and SHRobRDN (n=5). HMGB1 in arbitrary units (AU) normalized to GAPDH.

c) Representative Western blots (left panel) and assessment of phospho-NFkB/NFkB ratio (right panel) in left atrial homogenates from normotensive controls (n=5), SHR (n=6), SHRob (n=5) and SHRobRDN (n=5).

**p<0.05 versus Control; § p<0.05 versus SHR; #p<0.05 versus SHRob*

Fig. 4

a) Representative Western blot (upper panel) and quantification of membrane RAGE expression in cardiomyoblasts H9C2 (lower panel) repeatedly stimulated with isoproterenol (ISO) 0.1 umol/l (n=4) in the presence or absence of CGP (ß1-selective antagonist; 0.3 umol/l) or ICI (ß2-selective antagonist; 0.1 umol/l) for 72h every 24h. RAGE expression in arbitrary units (AU) with the control sample assigned a value of 1.

b) Representative Western blot (upper panel) and quantification of sRAGE secretion in cell culture medium of cardiomyoblasts H9C2 (lower panel) repeatedly stimulated with isoproterenol (ISO) 0.1 umol/l (n=4) in the presence or absence of CGP (ß1-selective antagonist; 0.3 umol/l) or ICI (ß2-selective antagonist; 0.1 umol/l) for 72 h every 24h. sRAGE expression in arbitrary units (AU) with the control sample assigned a value of 1.

**p<0.05 versus Control and ISO+CGP; #p<0.05 versus Control and ISO+ICI*

Figure 1

A

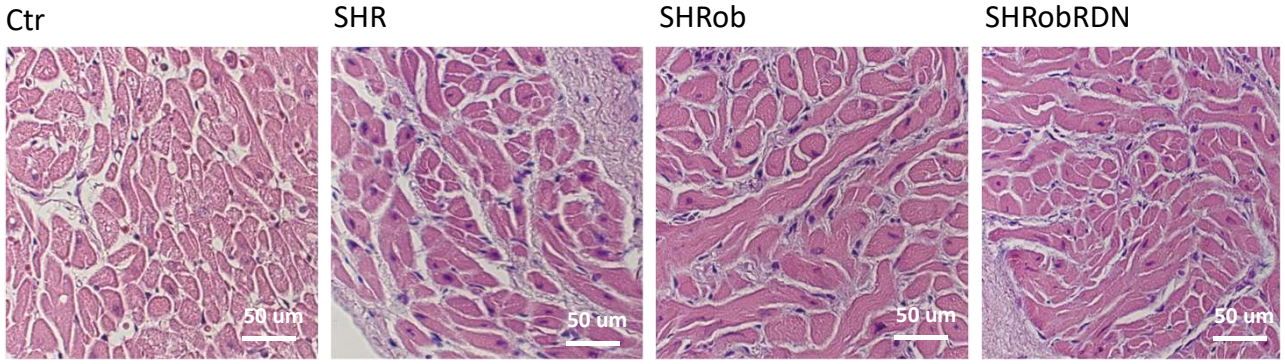
Ctr
SHR
SHRob
SHRobRDN
50 um
50 um
50 um
50 um

B

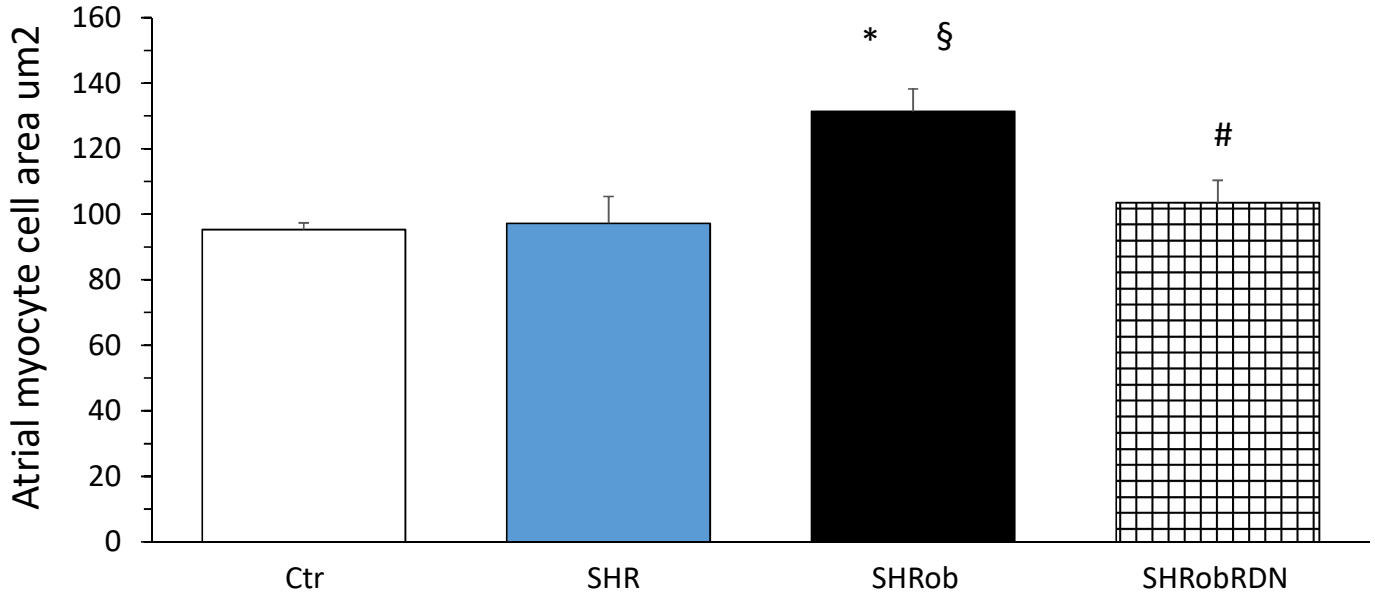
Atrial myocyte cell area um2
160
140
120
100
80
60
40
20
0
*
§
#
Ctr
SHR
SHRob
SHRobRDN

Figure 1

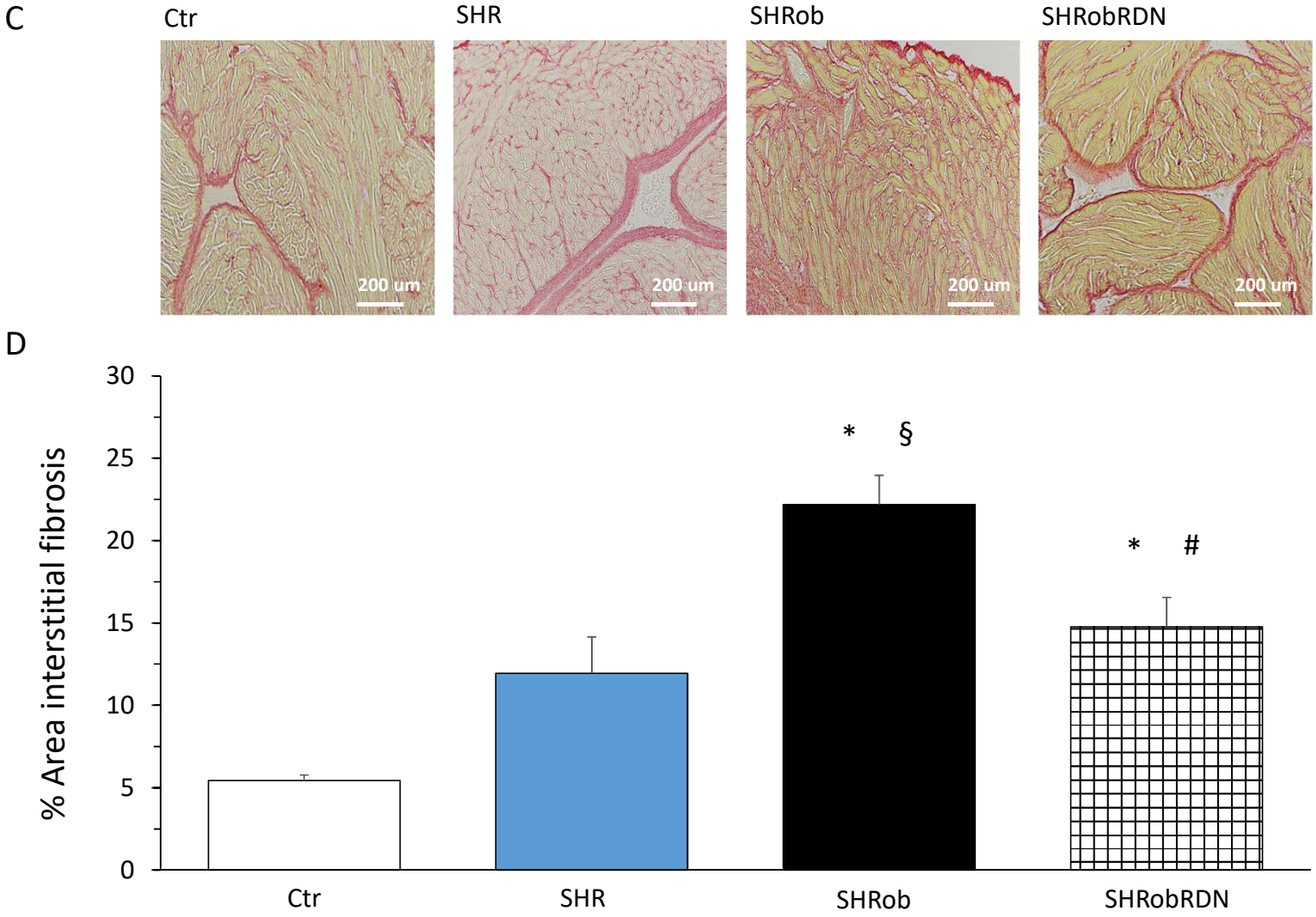
C
Ctr
SHR
SHRob
SHRobRDN
200 um
200 um
200 um
200 um
D
% Area interstitial fibrosis
30
25
20
15
10
5
0
* §
* #
Ctr
SHR
SHRob
SHRobRDN

Figure 1

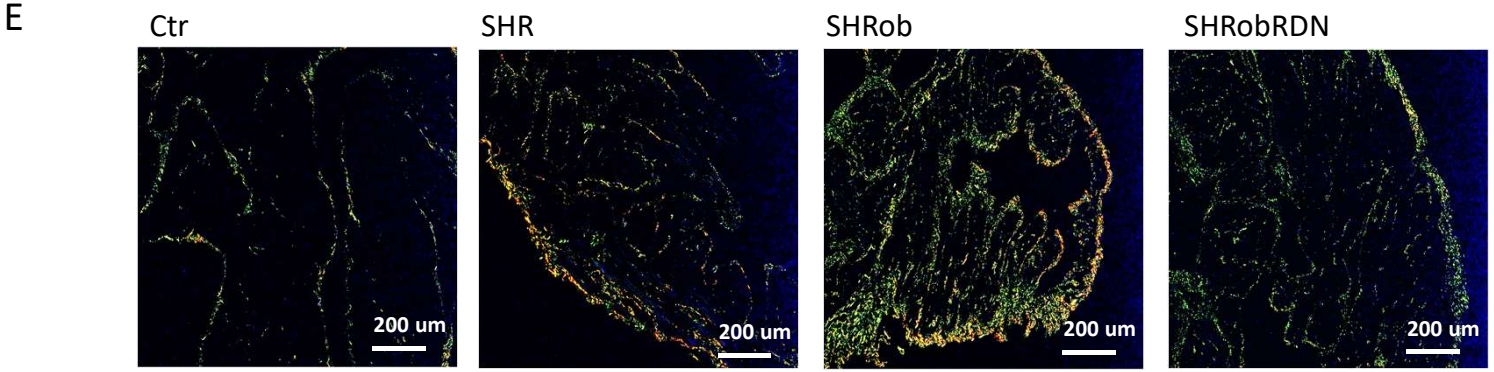
E
Ctr
SHR
SHRob
SHRobRDN
200 um
200 um
200 um
200 um

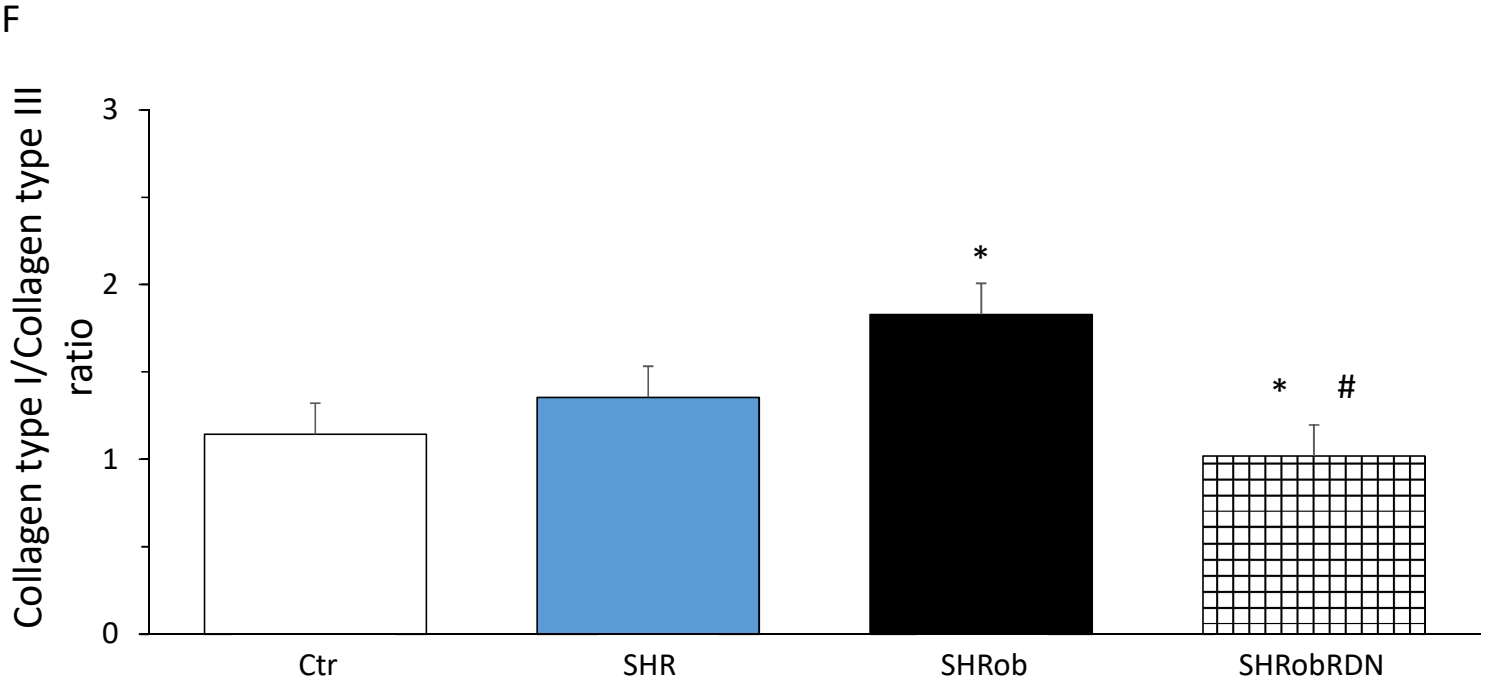
F
Collagen type I/Collagen type III ratio
3
2
1
0
*
* #
Ctr
SHR
SHRob
SHRobRDN

Figure 1

G

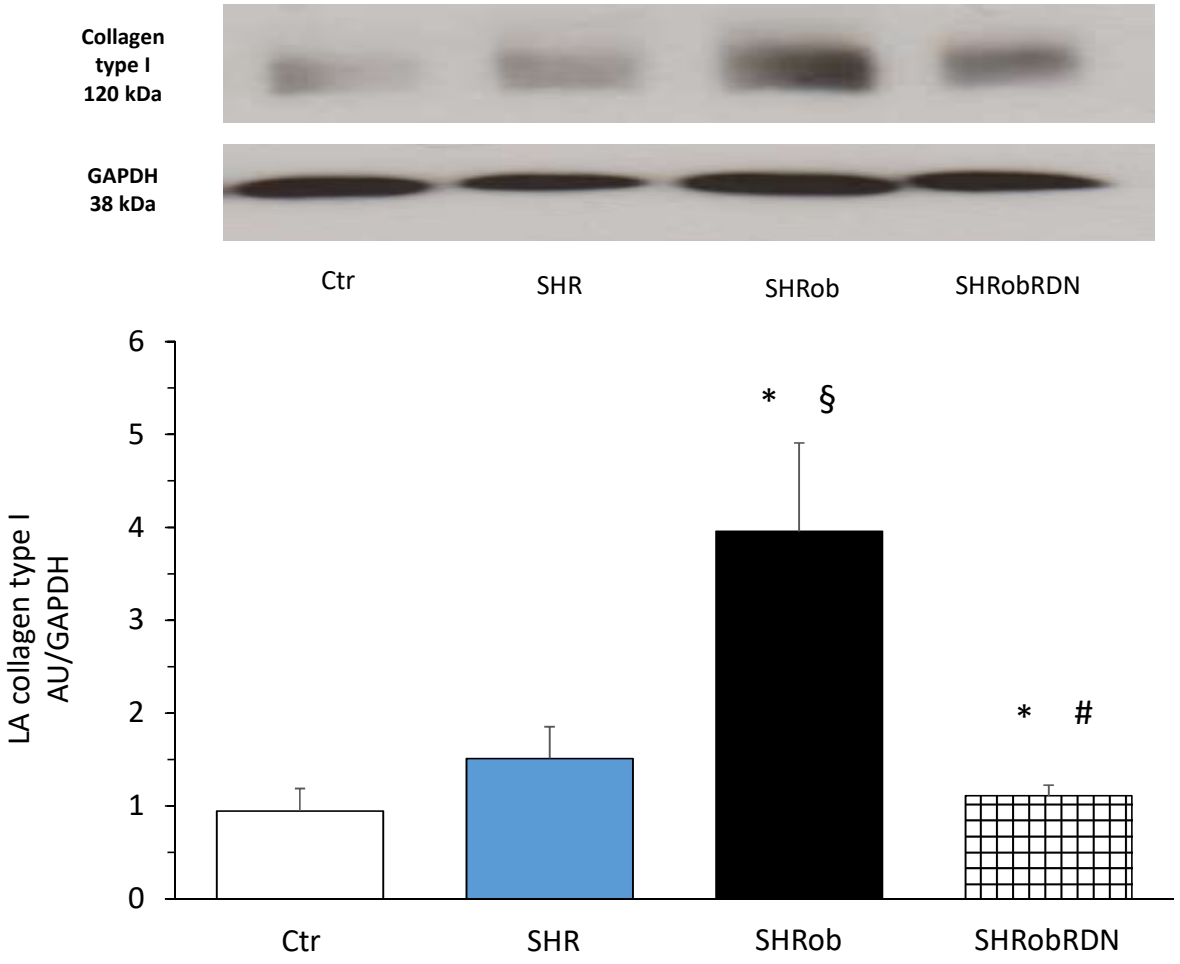
Collagen
type I
120 kDa
GAPDH
38 kDa
Ctr
SHR
SHRob
SHRobRDN
LA collagen type I
AU/GAPDH
6
5
4
3
2
1
0
*
§
*
#
Ctr
SHR
SHRob
SHRobRDN

Figure 2

A RAGE immunostaining

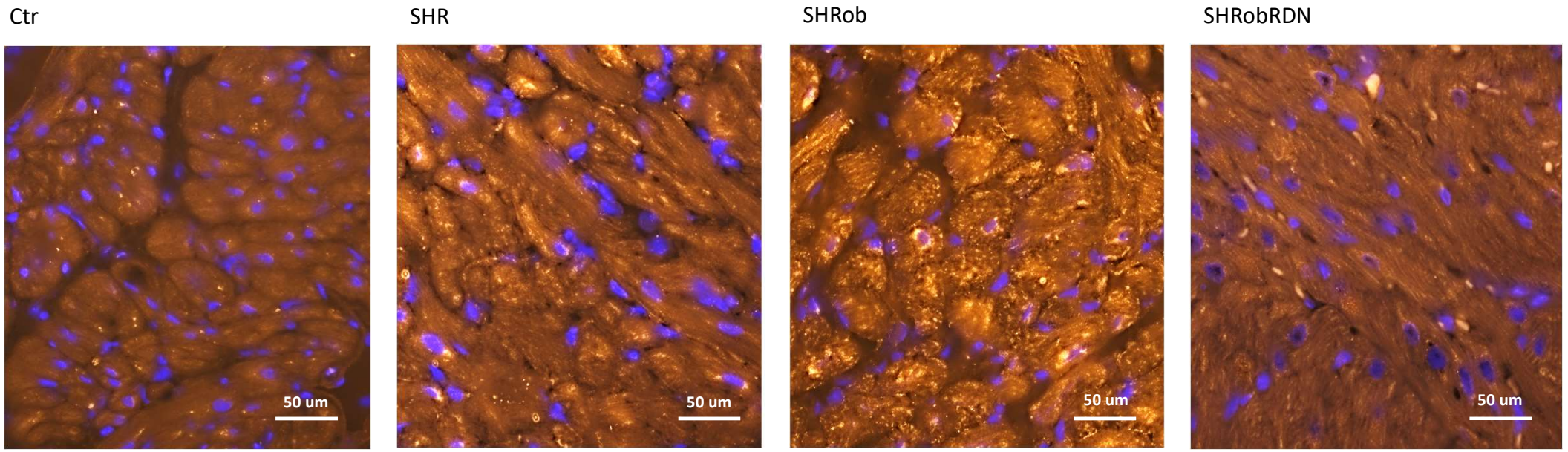

RAGE; autofluorescence; nuclei (DAPI)

Figure 2

B LA RAGE

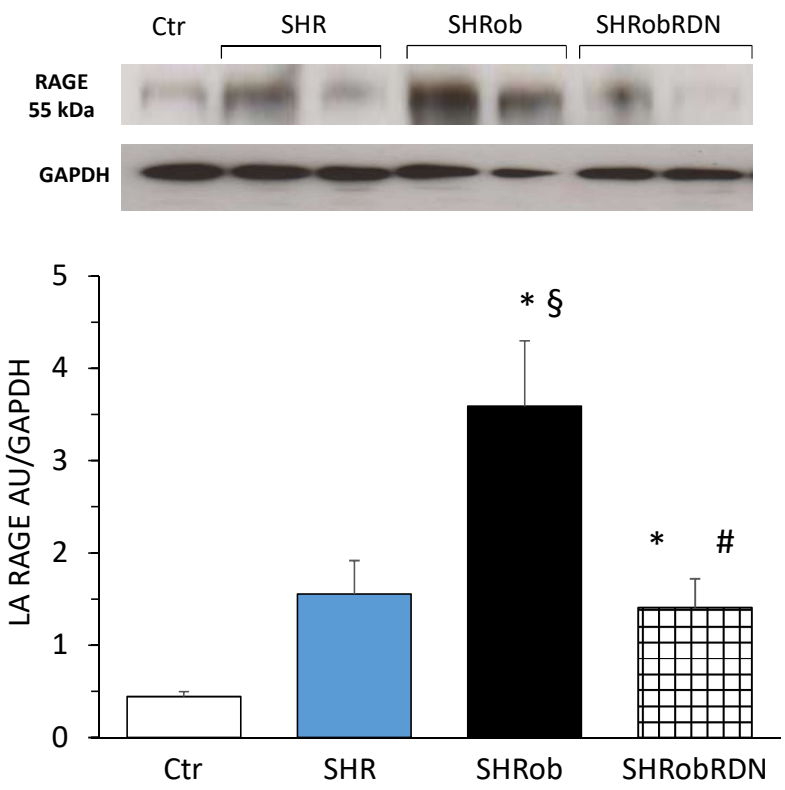

C LA sRAGE

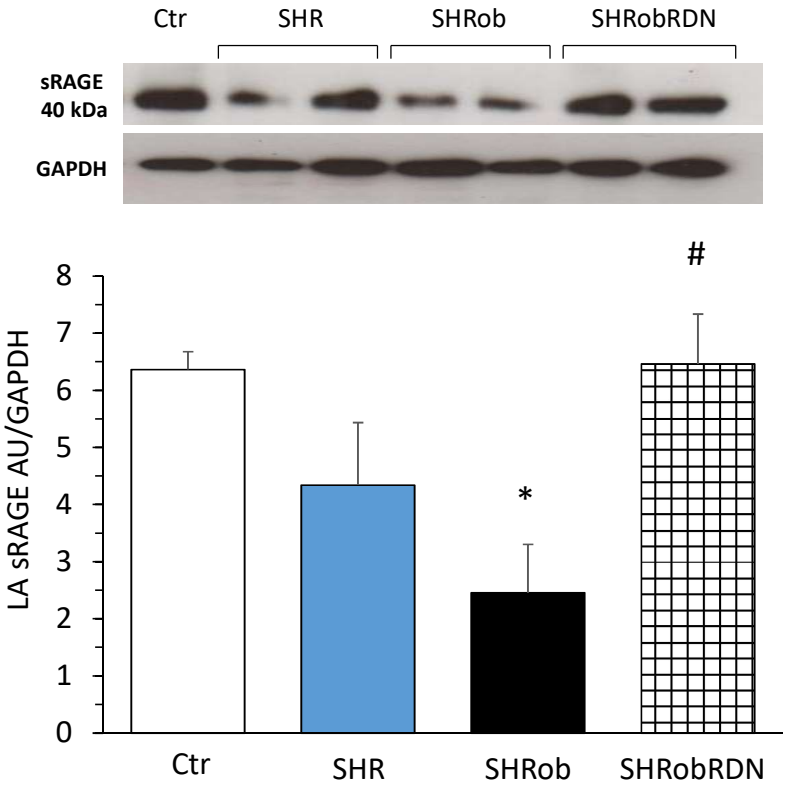

Figure 3

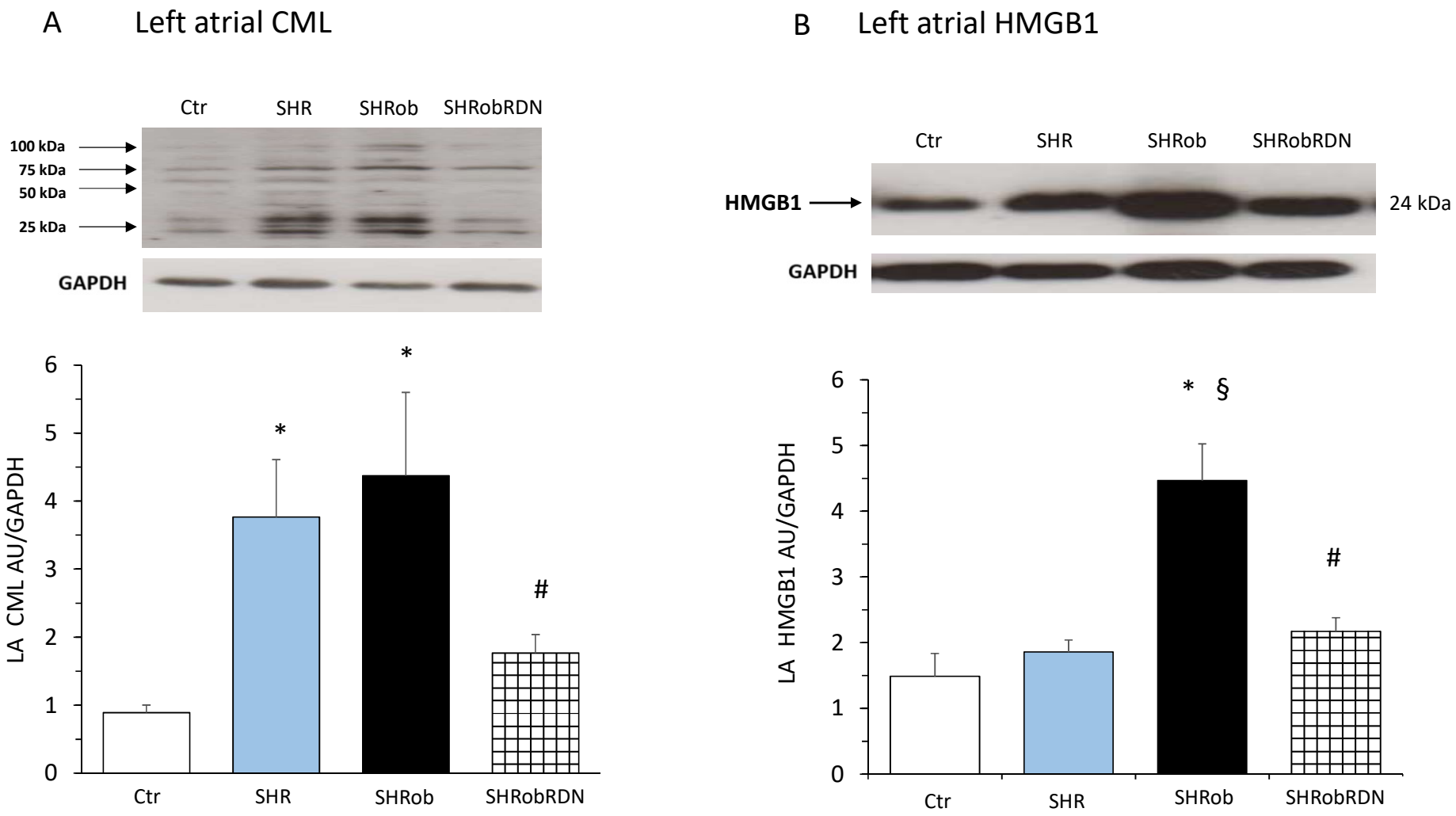
A Left atrial CML
Ctr
SHR
SHRob
SHRobRDN
100 kDa
75 kDa
50 kDa
25 kDa
GAPDH
LA CML AU/GAPDH
0
1
2
3
4
5
6
*
*
#
Ctr
SHR
SHRob
SHRobRDN
B Left atrial HMGB1
Ctr
SHR
SHRob
SHRobRDN
HMGB1
24 kDa
GAPDH
LA HMGB1 AU/GAPDH
0
1
2
3
4
5
6
* §
#
Ctr
SHR
SHRob
SHRobRDN

Figure 3

C Left atrial expression of NFkB

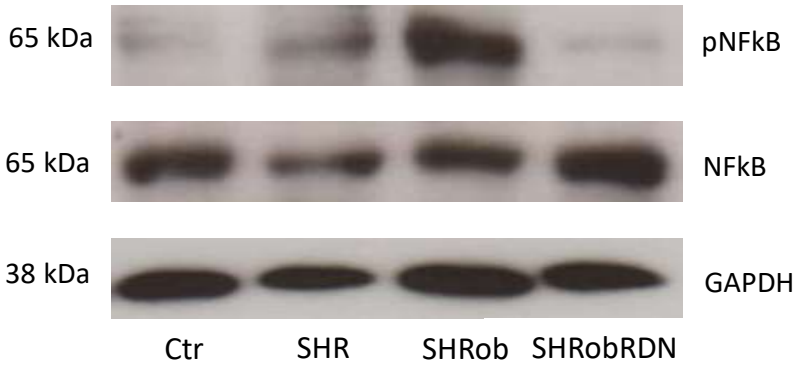

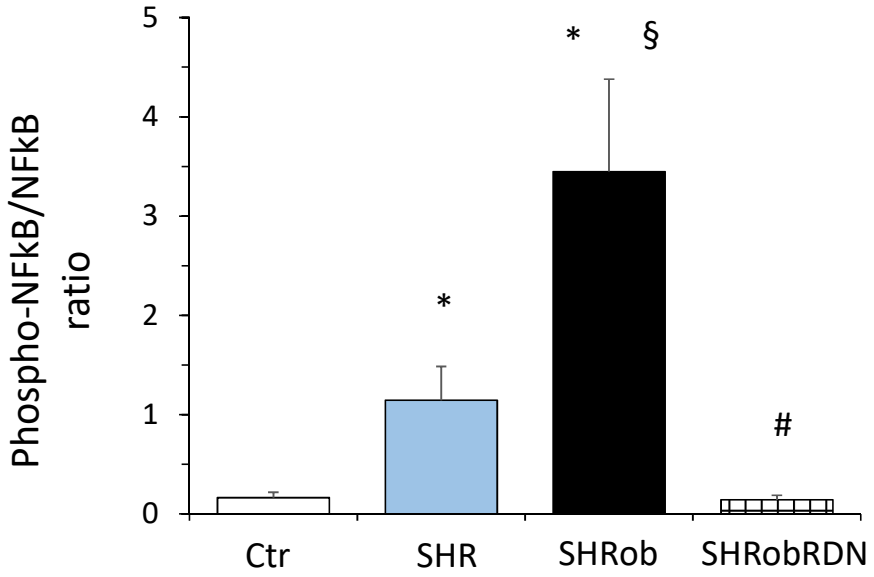

Figure 4 H9C2 cardiomyoblasts

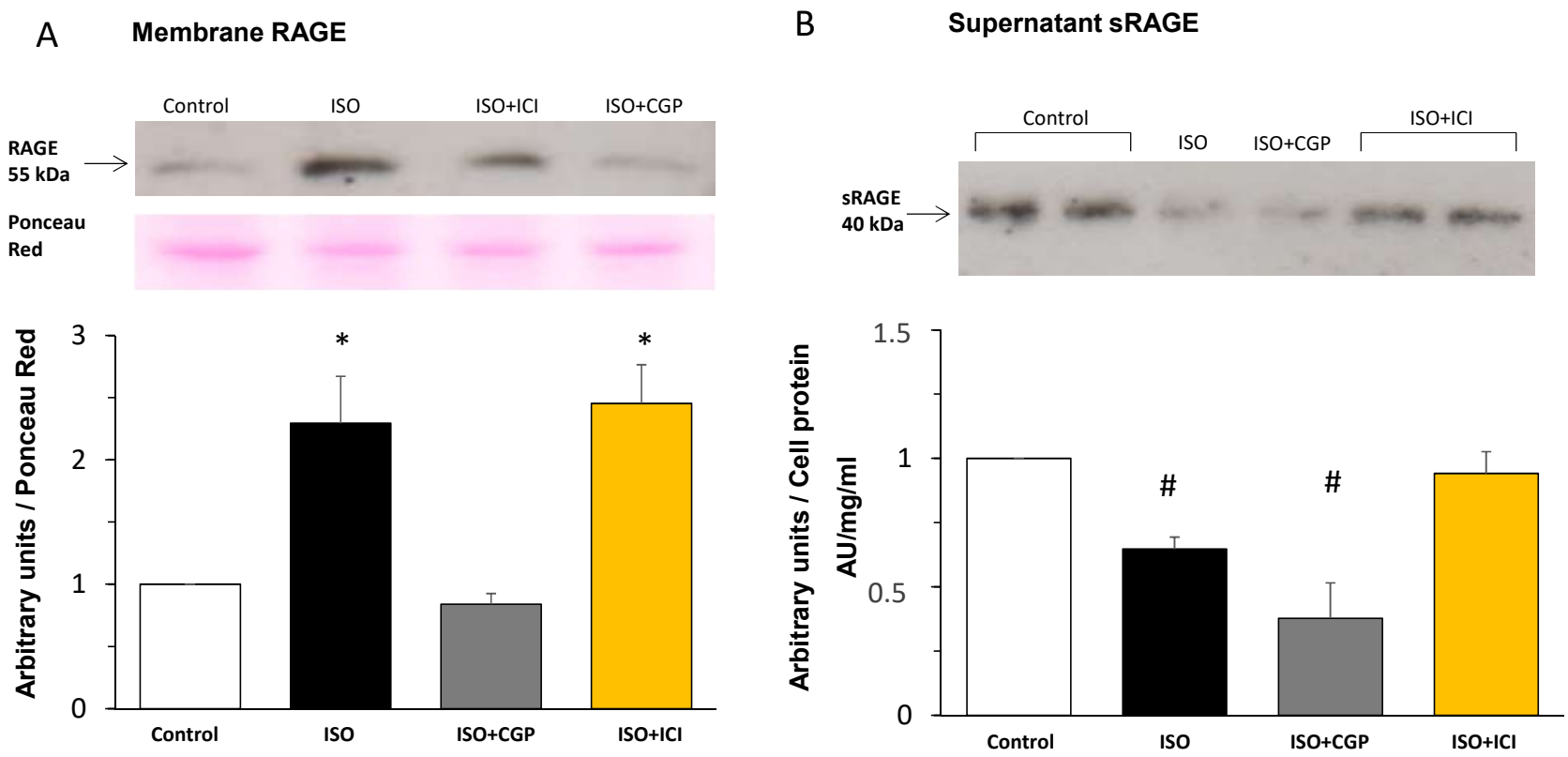

Table 1: Metabolic parameters, left atrial interstitial remodelling, RAGE/sRAGE, RAGE-ligands

	Controls N=5	**SHR N=5**	**SHRob N=5-6**	**SHRobRDN N=5-6**	**Ctrs vs. SHR**	**Ctrs vs. SHRob**	**Ctrs vs. SHRobRDN**	**SHR vs. SHRob**	**SHR vs. SHRobRDN**	**SHRob vs. SHRobRDN**
					p-values					
Body weight [g]	592±17	499±34	700±7	680±14	0.026	0.0095	0.037	<0.0001	<0.0001	n.s.
Mean systolic arterial blood pressure [mmHg]	118±10	190±6	220±6	185±10	<0.001	<0.001	<0.001	0.04	n.s.	0.01
Heart rate [bpm]	350±11	325±12	285±3	293±6	n.s.	0.0012	0.0033	0.036	n.s.	n.s.
Creatinine [umol/l]	16.2±1.7	25±1.8	30±0.9	19.6±2.9	0.02	0.0007	n.s.	n.s.	n.s.	0.008
HbA1c [%]	3.5±0.1	3.5±0.06	3.7±0.18	3.7±0.09	n.s	n.s	n.s	n.s	n.s	n.s
Fasting Insulin [pg/ml]	930±110	1245±412	9649±1679	8411±443	n.s.	<0.0001	<0.0001	<0.0001	0.0001	n.s.
Cholesterol [mmol/l]	4±0.2	3.7±0.23	9.5±0.2	9.3±0.3	n.s.	<0.0001	<0.0001	<0.0001	<0.0001	n.s.
Triglycerides [mmol/l]	1.7±0.09	1.7±0.2	5.8±0.2	5.5±0.2	n.s.	<0.0001	<0.0001	<0.0001	<0.0001	n.s.
Renal Norepinephrine [pg/ml]	85±3.6	97±1.5	98.4±10	6.97±2.6	n.s.	n.s.	<0.0001	n.s.	<0.0001	<0.0001
LA RAGE [AU/GAPDH]	0.4±0.1	1.6±0.4	3.6±0.7	1.4±0.3	n.s.	0.001	n.s.	0.02	n.s.	0.016
LA sRAGE [AU/GAPDH]	6.4±0.3	4.3±1.1	2.5±0.8	6.5±0.9	n.s.	0.04	n.s.	n.s.	n.s.	0.019
LA CML [AU/GAPDH]	0.9±0.1	3.7±0.7	4.6±0.9	2.0±0.3	0.04	0.005	n.s.	n.s.	n.s.	0.025
LA HMGB1 [AU/GAPDH]	1.5±0.4	1.8±0.1	4.5±0.6	2.2±0.2	n.s.	0.0003	n.s.	0.0006	n.s.	0.002
Collagen type I [AU/GAPDH]	0.9±0.2	1.5±0.3	4.0±1.0	1.1±0.1	n.s.	0.004	n.s.	0.02	n.s.	0.007
Collagen type I/collagen type III ratio	1.1±0.02	1.4±0.2	1.8±0.3	1.0±0.1	n.s.	0.04	n.s.	n.s.	n.s.	0.047
phosphoNFkB/ total NFkB ratio	0.16±0.04	1.1±0.3	3.4±0.9	0.14±0.05	n.s.	0.0013	n.s.	0.022	n.s.	0.0012
LA Interstitial Fibrosis [%]	5.5±0.3	12.6±1.8	22.2±1.8	14.8±1.8	0.03	<0.0001	0.0033	0.0024	n.s.	0.018
LA atrial myocyte cell area [um2]	95.8±1.6	97.2±8.2	130.5±5.4	100.8±3.4	n.s.	0.0013	n.s.	0.002	n.s.	0.005